



**Technical Report**  
RAL-TR-1999-008

# **Electron Acceleration in a Pre-Formed Plasma at 527nm**

**TMR Large-Scale Facilities Access Programme**

**F Amiranoff et al**



24<sup>th</sup> February 1999

**© Council for the Central Laboratory of the Research Councils 1999**

Enquiries about copyright, reproduction and requests for additional copies of this report should be addressed to:

The Central Laboratory of the Research Councils  
Library and Information Services  
Rutherford Appleton Laboratory  
Chilton  
Didcot  
Oxfordshire  
OX11 0QX  
Tel: 01235 445384 Fax: 01235 446403  
E-mail [library@rl.ac.uk](mailto:library@rl.ac.uk)

**ISSN 1358-6254**

Neither the Council nor the Laboratory accept any responsibility for loss or damage arising from the use of information contained in any of their reports or in any communication about their tests or investigations.

# **Electron acceleration in a pre-formed plasma at 527 nm**

**An experiment performed with funding from the  
TMR Large-Scale Facilities Access Programme**

**Access to Lasers at the Central Laser Facility Rutherford Appleton  
Laboratory Contract No. ERBFMGECT950053**

F Amiranoff, V Malka, M Salvati  
LULI, Ecole Polytechnique, Palaiseau, France

EL Clark, AE Dangor, K Krushelnick, A Modena, Z Najmudin, M Santala, M Tatarakis.  
Imperial College, Prince Consort Road, London, UK

C Clayton, D Gordon  
UCLA, Los Angeles, California, US

G Malka  
University of Orsay, France

D Neely, R Allott, JL Collier, C N Danson, A Djaoui, CB Edwards, P Flintoff, P Hatton,  
M Harman, MHR Hutchinson DA Pepler, IN Ross, T Winstone  
CLRC Rutherford Appleton Laboratory, Chilton, Didcot, Oxon, OX11 0QX. Email

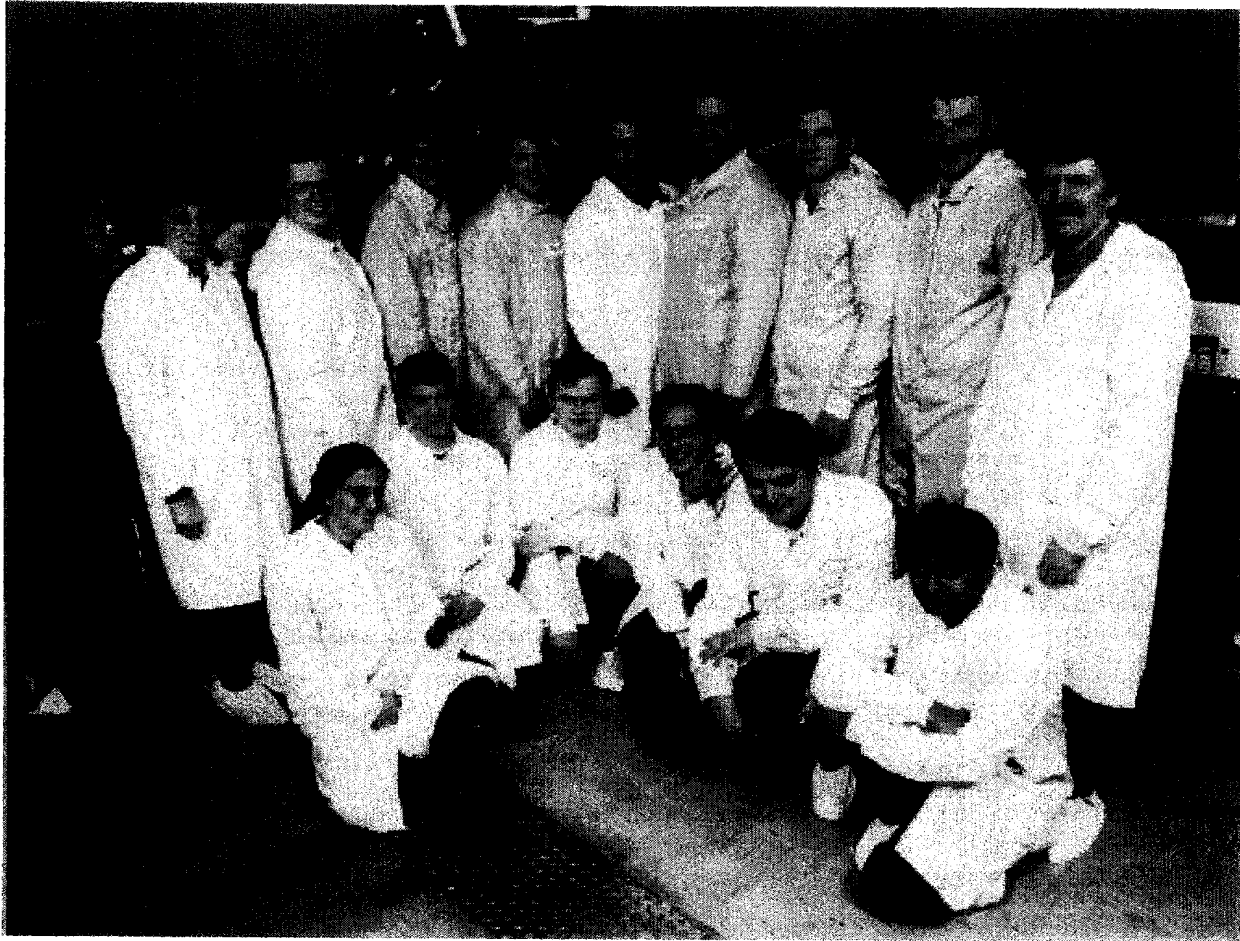
## SUMMARY

This report describes the experiment "Electron acceleration in a pre-formed plasma at 527 nm."; carried out at the Central Laser Facility (CLF) from the 5<sup>th</sup> Jan to the 14<sup>th</sup> Feb 1998. The experiment, funded by the Framework IV Large Scale Facilities access scheme, was proposed by Dr F Amiranoff, LULI, Ecole Polytechnique, France and carried out by visiting researchers from the Laboratory. They were supported by researchers from: Imperial College, London, UK; UCLA, Los Angeles, California, US; University of Orsay, France; and the Central Laser Facility, Rutherford Appleton Laboratory.

## Experimental Results

- The experiment was the first quantitative study of Forward Raman Scattering (FRS) at 527 nm, interesting in its own right, but also a fundamental mechanism for electron acceleration
- FRS was shown to be very efficient at the second harmonic giving higher phase velocities at 527 nm compared to fundamental interactions at 1053 nm
- Efficient frequency doubling of Vulcan's large aperture CPA beam was successfully demonstrated for the first time with pulses of >10 TW being delivered to target

*The CLF makes beam time at its facilities available to European Researchers with funding from DG-XII, CEC under the Large-Scale Facilities Access Scheme. For further information contact Dr. Chris Edwards at the CLF. Tel: (0)1235 445582, e-mail: c.b.edwards@rl.ac.uk*



The experimental team from Ecole Polytechnique, collaborators from Imperial College, London, and UCLA, California and support staff from RAL

From left to right:

Top row: N Prior, D Neely, CN Danson, P Fintoff, K Krushelnik, R Allott,  
D Pepler, CB Edwards and P Griffiths

Bottom row: M Salvati, D Gordon, M Santala, V Malka, M Tatarakis, Z Najmudin

## **Arising Publications**

### **Refereed Publications and Conference Proceedings**

D Neely, CN Danson, R Allott, F Amiranoff, EL Clark, C Clayton, JL Collier, AE Dangor, A Djoui, CB Edwards, P Flintoff, D Gordon, MHR Hutchinson, K Krushelnick, G Malka, A Modena, Z Najmudin, DA Pepler, IN Ross, A Santala, M Tatarakis, M Trentelman and T Winstone. "Multi Terawatt Frequency Doubling of Picosecond Pulses for Plasma Interactions." Submitted to SPIE, Monterey 1998.

D Neely, CN Danson, R Allott, JL Collier, CB Edwards, P Flintoff, MHR Hutchinson, DA Pepler, IN Ross, M Trentelman, T Winstone, Z Najmudin, V. Malka, F Amiranoff, EL Clark, AE Dangor, D Gordon, K Krushelnick, G Malka, A Modena, M Salvati, M Santala, and M Tatarakis. "Multi Terawatt Frequency Doubling Of Picosecond Pulses For Plasma Interactions." Accepted to Lasers and Particle Beams

Z Najmudin, V Malka, R Allott, F Amiranoff, EL Clark, AE Dangor, CN Danson, P Flintoff, D Gordon, C Joshi, K Krushelnick, G Malka, A Modena, D Neely, M Salvati, M Santala and M Tatarakis. 'Studying Forward Raman Scattering with a multi-terawatt 527 nm laser beam.' Paper in preparation.

### **Conference presentations**

*XXV ECLIM, Formia, Italy, 4-8 May 1998.*

D Neely, CN Danson, R Allott, JL Collier, CB Edwards, P Flintoff, MHR Hutchinson, DA Pepler, IN Ross, M Trentelman, T Winstone, Z Najmudin, V. Malka, F Amiranoff, EL Clark, AE Dangor, D Gordon, K Krushelnick, G Malka, A Modena, M Salvati, M Santala, and M Tatarakis. "Multi Terawatt Frequency Doubling Of Picosecond Pulses For Plasma Interactions."

Z Najmudin, V Malka, R Allott, F Amiranoff, EL Clark, AE Dangor, CN Danson, P Flintoff, D Gordon, C Joshi, K Krushelnick, G Malka, A Modena, D Neely, M Salvati, M Santala and M Tatarakis. "High Intensity Laser Interactions with a Gas Jet."

M Salvati, R Allott, F Amiranoff, EL Clark, AE Dangor, CN Danson, P Flintoff, D Gordon, K Krushelnick, V Malka, G Malka, A Modena, Z Najmudin, D Neely, M Santala and M Tatarakis. "High Intensity Laser Interactions with a Gas Jet at 527 nm."

# Studying Forward Raman Scattering with a multi-terawatt 527 nm laser beam

## Introduction

The emergence of high-power short pulse lasers around the world has generated interest in the interaction of high intensity laser light with plasmas. In particular it has allowed for a better study of the Forward Raman Scatter (FRS) instability. FRS has long been studied in connection with laser driven inertial confinement fusion studies, since a by-product of FRS is the generation of a high amplitude plasma wave<sup>1</sup>. This plasma wave can accelerate plasma electrons, which can have the undesirable effect on direct drive ICF capsules of pre-heating the capsule core, leading to shorter confinement times. Studies of FRS close to the quarter critical surface of a solid-laser interaction<sup>2</sup>, where the growth rate is greatest, tend to be incomplete since it is impossible to identify the FRS directly (through optical measurements) as the cause of the excessive electron heating. Theoretical calculations of the growth rate of FRS indicate that the growth of the instability maximizes for incident electromagnetic radiation with a normalized vector potential  $a_0 \approx 1$ <sup>3, 4</sup>. (The vector potential of a laser beam of frequency  $\omega$  is given by

$$a_0 = eE_{\text{laser}}/m_e \omega c$$

Hence novel short pulse lasers which allow the intensities required for this kind of vector potential, opportune more systematic studies of this instability, which can be performed at lower densities. Indeed many studies have been performed with high power Nd:Glass laser systems at a wavelength of 1  $\mu\text{m}$ , that clearly show the action of Forward Raman scatter in modulating the laser at multiples of the plasma frequency, so generating a spectrum with satellite lines separated from the fundamental by multiples of the harmonic frequency<sup>5-8</sup>. Also observed has been the production of copious quantities of suprathermal energy electrons. These electrons are produced when the plasma wave generated by the FRS decays through wavebreaking. Electrons with energies of up to 94 MeV<sup>9</sup> and a beam of electrons of energy greater than 1 MeV with a normalized emittance as low as 0.4  $\pi$  mm mrad<sup>8</sup> have been observed. The latter figure is an order of magnitude brighter than comparable state-of-the-art photo-injectors. Hence FRS can be an interesting high brightness source of moderately relativistic electrons. That acceleration can take place to such high energies, is a result of the high phase velocity of the accelerating electric field of the plasma wave. Indeed since the plasma wave must be in phase with modulations of the laser pulse energy for the wave to grow, the phase velocity of the plasma wave is equal to the group velocity of light in the plasma. For plasma frequency  $\omega_p$  much less than the laser frequency  $\omega_0$ , the Lorentz factor of the plasma wave  $\gamma_\phi \approx \omega_0/\omega_p$ . Hence one can see that for a greater  $\omega_0/\omega_p$ , the greater the maximum acceleration. A simple estimate of the maximum acceleration energy is given by  $W_{\text{max}} = 2\pi\gamma_\phi^2 m_e c^2 \epsilon^{1/2}$  (1), where  $\epsilon$  is the ratio of plasma wave density variations

to initial plasma density<sup>10</sup>. This estimate was exceeded in experiments performed with 1  $\mu\text{m}$  laser light at densities around  $10^{19}\text{cm}^{-3}$ , to give accelerated electron energies up to 94 MeV<sup>9</sup>. It is found in simulation, that this is due to a second stage acceleration where the large current of accelerated electrons which outrun the plasma wave, can set up a (non-resonant) higher phase velocity plasma perturbation, which itself can accelerate the tail of this accelerated bunch to yet higher energies<sup>11</sup>. However to a first approximation it can be seen that increasing the phase velocity of the plasma wave, either by reducing density or by increasing the driver pulses frequency, can lead to an increase in maximum acceleration energy. Figure 1 shows the gain of FRS for a 1 ps square pulse as a function of intensity for a 1  $\mu\text{m}$  driver beam at a density of  $1\cdot 10^{19}\text{cm}^{-3}$ . This is the density close to which wavebreaking is observed in previous experiments performed a 1  $\mu\text{m}$ . Also plotted on the same graph is the gain with a 0.5  $\mu\text{m}$  driver beam at a range of different densities. One notices that it is possible to obtain the same growth by an increase in density at the same intensity. From the graph, one sees that at intensities less than  $1\cdot 10^{18}\text{Wcm}^{-2}$ , it is possible to match the growth rate at 1  $\mu\text{m}$  by an almost three-fold increase in density at 0.5  $\mu\text{m}$ , or a  $\sqrt{3}$  increase in plasma-frequency. Since the Lorentz factor  $\gamma_\phi$  of the FRS created plasma wave is proportional to  $\omega_0/\omega_p$ , doubling the driver frequency results in an increase in phase velocity as well as a moderate increase in maximum possible accelerated energy of 4/3. At intensities close to  $1\cdot 10^{18}\text{Wcm}^{-2}$ , the FRS growth for 1  $\mu\text{m}$  saturates since at this intensity  $a_0$  is close to 1, (the maximum is actually  $a_0 \approx 1.4$ ). This is a result of the relativistic mass increase of the electrons quivering in the laser electric field at these intensities, which serves to reduce the effective plasma frequency. However for 0.5  $\mu\text{m}$ , the FRS growth rate does not

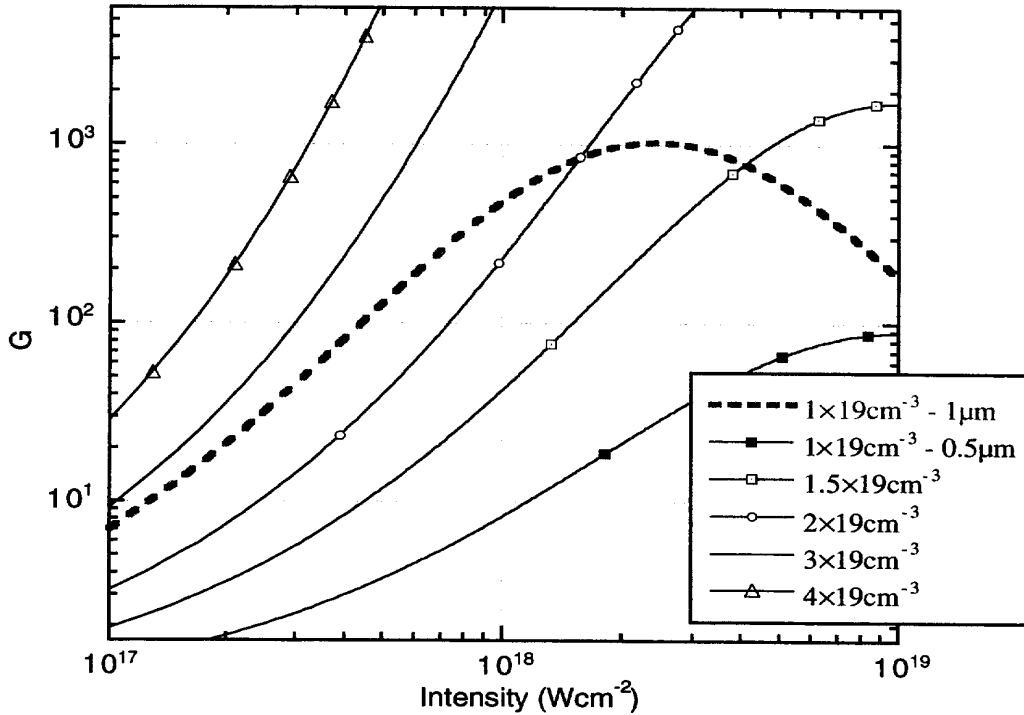


Figure 1. Gain of FRS for either 1  $\mu\text{m}$  at  $n_e=1\cdot 10^{19}\text{cm}^{-3}$  or 0.5  $\mu\text{m}$  at a variety of densities as a function of intensity



reach its maximum until intensities close to  $1 \cdot 10^{19} \text{ Wcm}^{-2}$ . Hence it is possible to obtain equivalent growth rates at almost the same densities, resulting in yet higher maximum acceleration energies. Indeed we can see that the same growth rates can be obtained at densities only slightly greater than that required for wave-breaking at  $1 \mu\text{m}$ . Hence frequency doubling of a high intensity laser beam can be of interest when using short pulses as drivers for plasma based source of high-energy particles.

## II. Experiment

The experiment was performed with the Vulcan CPA laser<sup>12</sup>. This produces up to 30 J of infra-red energy at  $1 \mu\text{m}$ , in a stretched large bandwidth pulse. The pulse was recompressed with a pair of gold coated gratings. For these studies at 527 nm requires the Vulcan CPA beam to be frequency doubled. Appendix 1 of this report details the characterization tests conducted to provide this new illumination option which gave up to 9 J at 527 nm in a 700 fs pulse. This high power beam is transported in vacuum and focused with a  $f5$  off-axis parabola, to a focal spot of  $30 \mu\text{m}$  diameter, thus giving an on-axis intensity of around  $1 \cdot 10^{18} \text{ Wcm}^{-2}$ . The spot is 6 times the diffraction limit at this wavelength. This is due to the greater than optimum thickness of the crystal used 4 mm for such a high intensity pulse<sup>13</sup>. The beam was focused to the edge of a supersonic helium gas jet. A supersonic gas jet is used to give a sharp vacuum gas interface, so as to prevent ionization induced defocusing becoming problematic before focus<sup>14, 15</sup>. The primary diagnostics were monitoring of the transmitted laser

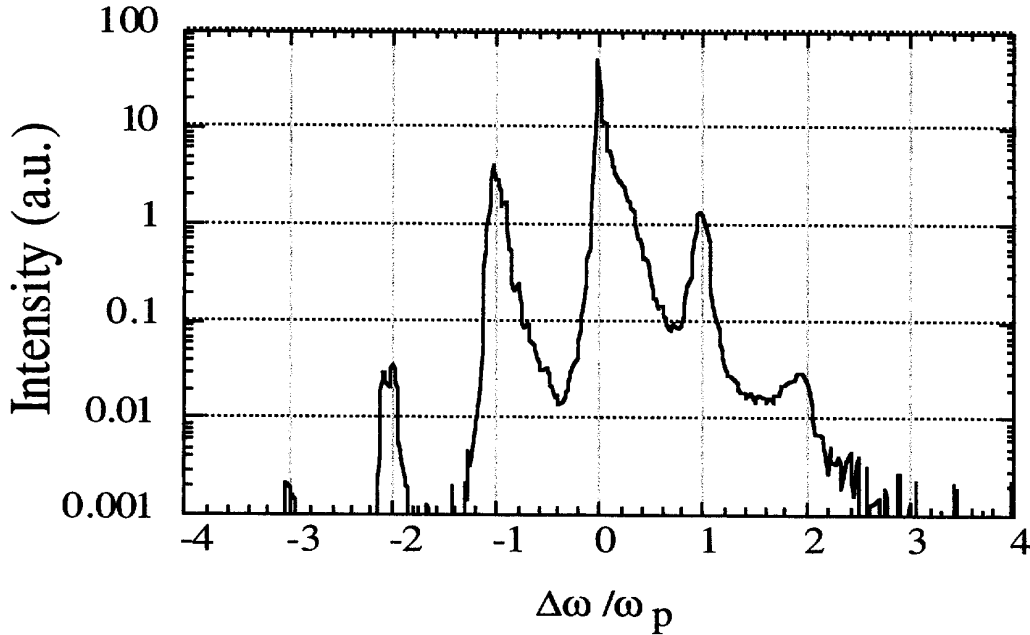


Figure 2. Typical FRS spectra showing cascading. Plasma density was  $4.4 \cdot 10^{19} \text{ cm}^{-3}$ , average  $|a_0|=0.32$ .

grow but slightly off-axis so that the downshifted satellite still dominates – and finally to the resonant four-wave – where both red satellite and blue satellite should grow with equal amplitude<sup>3, 4, 18, 19</sup>. Indeed that is what is seen in figure 3, in which increases in density - which cause increased growth rate, and so allow us to vary the rate of transition between these regimes - show the emergence of the blue shifted satellite in comparison to the red.

Indeed at densities greater than  $7 \cdot 10^{19} \text{ cm}^{-3}$ , one sees that the blue satellite is actually greater in amplitude than the red satellite. This is remarkable, because as we have said above in the early stages of the instability we expect the red satellite to dominate, but even in the four wave resonant regime we would expect that at best both satellites would have the same amplitude. Further evidence of this temporal transition is apparent in the spectrum shown in figure 2. As can be seen the laser light transmitted at the fundamental frequency, has an extended width to the blue side. This as has been reported by many authors is the result of ionization. The extremely high ionization rates, which are experienced in these interactions, result in a dramatic increase in density and a corresponding decrease in refractive index. This decreasing refractive index serves to retard the front of the pulse, causing a bunching of laser energy, and hence a blue shifting<sup>14, 15</sup>. In these experiments a helium gas jet was employed, which is ionized in two stages, the upper of which is fully ionized at an intensity of around  $1 \cdot 10^{16} \text{ Wcm}^{-2}$ . Hence one expects that most of the ionization and hence ionization-induced blue shifting will take place early in the pulse, as soon as this intensity is reached. Noticeably in figure 2, the red shifted satellite has a blue shift similar to the fundamental frequency profile. No such corresponding blue shifted tail is seen in the blue satellite. It is evident therefore that the red satellite is dominant early in the pulse, either scattering from the already blue shifted part of the driver pulse or being blue shifted itself due to the ongoing ionization at that time. The blue satellite only achieves prominence later into the pulse, when the ionization has been completed, and so does not exhibit this feature.

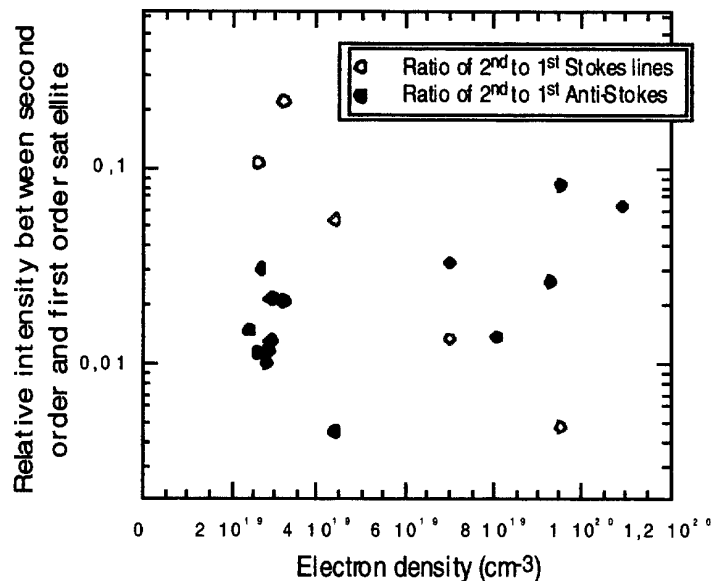


Figure 4. Ratio of 2<sup>nd</sup> to first 1<sup>st</sup> Stokes and Anti-Stokes lines as a function of density

Also noticeable in the spectra is the presence of satellites at multiples of the plasma frequency. This cascading of laser energy is a sign of feedback between the scattered electromagnetic waves and the plasma. Hence one can treat increasing signal of the higher  $\omega_p$  harmonics as a measure of increasing plasma wave amplitude. Figure 4 shows the ratio of the second to first satellites for both blue and red sides of the fundamental. On the red side there is a gradual exponential increase in this ratio, which as expected shows the distribution of energy to the higher harmonics as the created wave, and hence the non-linear feedback becomes larger. However on the blue side the behavior is completely different. Indeed the ratio of the second satellite to first actually decreases. This is in some part be due to the fact that, as commented before, the first blue satellite grows much more rapidly than the others. However it is noticeable that the second satellite does not seem to change in amplitude with increasing density. This implies that the cascading process is much more efficient for satellites of decreasing photon energy.

One can make a simple estimate of the plasma wave amplitude, if one assumes that the ratio of the harmonic Raman satellites is proportional to the harmonic content of the scattering plasma wave. This supposes that the generated sideband acts as a Thomson scattering probe for the self-generated plasma wave. This approach will overestimate the size of the plasma wave, because of the stimulated nature of the interaction. However it is countered by the fact that the final plasma wave amplitude is more than the average scattering amplitude. The harmonic amplitude of the scattering  $\mu_m$  as a function of the plasma wave amplitude  $\partial n/n_0$ , is given by,

$$(\mu_m/\mu_0)=(m^m/2^{m-1} \cdot m!) \cdot (\partial n/n_0)^m,$$

where  $m$  is the number of the harmonic. Hence the ratio between second and first harmonics is simply equal to the plasma wave amplitude. Figure 5 shows the value of the second to first Stokes line of the Raman signal. Values up to 0.03 were measured within our experimental parameters, implying plasma wave amplitudes of the same magnitude. Plotted against this value, is the total electron signal measured above 5 MeV (in arbitrary units) for a fixed setting of the dispersing magnet. One can see, as expected, that as the implied plasma wave amplitude becomes larger, so the total number of electrons trapped and accelerated becomes larger too. It is difficult to compare these results with those at other magnet settings since at these low energies, the dispersion of the electrons is adversely affected by scattering in air and in the thin mylar window through which the electrons beam is transported out of vacuum. However through the careful use of copper shielding in front of the detectors it is possible to eliminate lower energy electrons in the higher energy channels. With this method of shielding low energy electron noise, the maximum electron energy measured with these parameters was 18 MeV. For this particular shot the measured plasma wave amplitude was 0.02 and the density  $9 \cdot 10^{19} \text{ cm}^{-3}$ . With these parameters one can estimate the maximum energy of trapped electrons out-running the plasma wave. Using equation (1), one obtains an expected maximum energy of 19 MeV, well in line with the measured value. Though the numbers of electrons accelerated

to the highest energies is very small, it does seem that plasma wave acceleration is the mechanism in action here. Of course the fact that background electrons can be trapped and accelerated at plasma wave amplitudes well below the wave breaking limit<sup>1</sup> suggests that the plasma is extremely hot (~keV)). As has been explained elsewhere it is suggested that it is the influence of lower phase velocity stimulated scattering (in particular Raman back-scatter) that can provide the heating sufficient to allow these electrons to be trapped<sup>20, 21</sup>.

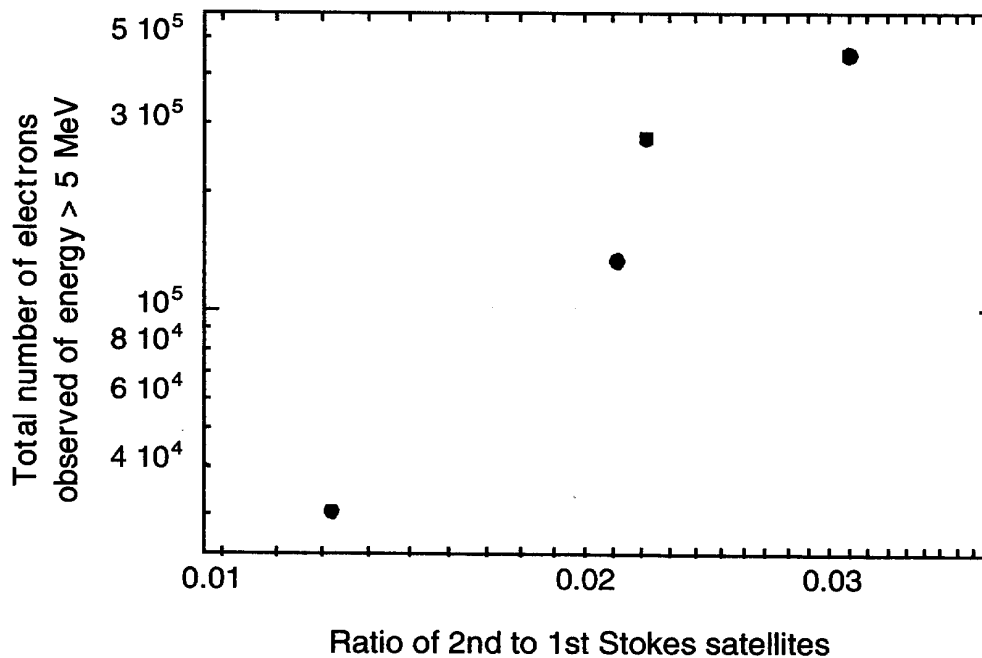


Figure 5 Total number of detected electrons versus the total number of electrons detected

## REFERENCES

- 1 A. Modena, Z. Najmudin, A. E. Dangor, *et al.*, *Nature* **377**, 606-608 (1995).
- 2 C. Joshi, T. Tajima, J. M. Dawson, *et al.*, *Phys Rev Lett* **47**, 1285-1288 (1981).
- 3 T. M. Antonsen and P. Mora, *Phys Rev Lett* **69**, 2204 (1992).
- 4 W. B. Mori, C. D. Decker, D. E. Hinkel, *et al.*, *Phys Rev Lett* **72**, 1482 (1994).
- 5 C. A. Coverdale, C. B. Darrow, C. D. Decker, *et al.*, *Phys Rev Lett* **74**, 4659-4662 (1995).
- 6 A. Modena, Z. Najmudin, A. E. Dangor, *et al.*, *IEEE Transactions On Plasma Science* **24**, 289-295 (1996).
- 7 A. Ting, C. I. Moore, K. Krushelnick, *et al.*, *Physics of Plasmas* **4**, 1889-1899 (1997).
- 8 R. Wagner, S. Y. Chen, A. Maksimchuk, *et al.*, *Phys Rev Lett* **78**, 3125-3128 (1997).

- 9 D. Gordon, K. C. Tzeng, C. E. Clayton, *et al.*, Phys Rev Lett **80**, 2133-2136 (1998).
- 10 E. Esarey, P. Sprangle, J. Krall, *et al.*, IEEE Transactions On Plasma Science **24**, 252-288 (1996).
- 11 K. C. Tzeng and W. B. Mori, , 1998).
- 12 C. N. Danson, J. Collier, D. Neely, *et al.*, Journal of Modern Optics **45**, 1653-1669 (1998).
- 13 D. Neely, C. N. Danson, R. Allott, *et al.*, in *ECLIM*, Formia, Italy, 1998).
- 14 A. J. Mackinnon, M. Borghesi, A. Iwase, *et al.*, Phys Rev Lett **76**, 1473-1476 (1996).
- 15 S. C. Rae, Optics Communications **104**, 330-335 (1994).
- 16 H. A. Enge, in *Focusing of Charged Particles*, edited by A. Septier (Academic, New York, 1977), p. ch. 4.2.
- 17 J. J. Livingood, *The Optics of Dipole Magnets* (Academic, New York, 1969).
- 18 S. Guerin, G. Laval, P. Mora, *et al.*, Physics of Plasmas **2**, 2807-2814 (1995).
- 19 C. J. McKinstrie and R. Bingham, Physics of Fluids B **4**, 2626 (1992).
- 20 E. Esarey, B. Hafizi, R. Hubbard, *et al.*, Phys Rev Lett **80**, 5552-5555 (1998).
- 21 K. C. Tzeng and M. W. B., Phys Rev Lett **81**, 104-107 (1998).

# **Appendix 1**

## **Multi-terawatt Frequency Doubling of Picosecond Pulses for Forward Raman Scattering Interactions**

### **Introduction**

An investigation was carried out to select the optimum scheme for frequency doubling the 1054 nm sub picosecond Vulcan chirped pulse amplified (CPA) beam for a Forward Raman Scattering experiment. A 4 mm thick Type I KDP crystal was selected and during the experiment a frequency doubled beam line was commissioned and delivered pulses of over 10 TW onto target. This appendix describes the selection of the crystal and the characterisation of the resultant frequency doubled beam.

### **Doubling Efficiency**

In order to determine the most appropriate crystal length and operating intensity regime for the large aperture CPA beam, a number of frequency doubling conversion efficiency measurements were carried out on small 25 mm diameter aperture KDP crystals. The crystal lengths were 2 and 4 mm and were operated at a range of incident intensities up to 300 GWcm<sup>-2</sup>. To ensure high contrast ratio on the target it is essential to eliminate any unconverted fundamental component in the final beam. Type I frequency conversion was used for these experiments which produces orthogonally polarised fundamental and second harmonic components. These orthogonally polarised components are relatively easy to separate using polarisation sensitive reflective mirrors.

The incident infrared and converted green beam energy was measured using absorption calorimeters. The data is presented in figure 1. The majority of the data was obtained using a 1 ps CPA pulse, although a number of points were obtained using a 2.5 ps YLF pulse. The data shows that a 4 mm crystal gives optimum conversion efficiency at an irradiance of ~150 GWcm<sup>-2</sup> and the optimum conversion efficiency for a 2 mm thick crystal is at an intensity greater than 250 GWcm<sup>-2</sup>. The lines in the figure are fits to all of the conversion efficiency data points using a power series expansion in  $IL^2$ , where  $I$  is the intensity and  $L$  the crystal thickness. Frequency doubling was theoretically examined by Armstrong<sup>7)</sup> where conversion efficiency was shown to scale as a function of  $IL^2$ . However, when calculating the conversion efficiency, Armstrong did not include the effects of the intensity dependent refractive index change, as this effect was negligible in the range he considered. In our measurements significant intensity dependent refractive index changes are present and therefore preclude us from using a simple fit to  $IL^2$ . Thus, a single polynomial function,  $C(I,L)$  of the form

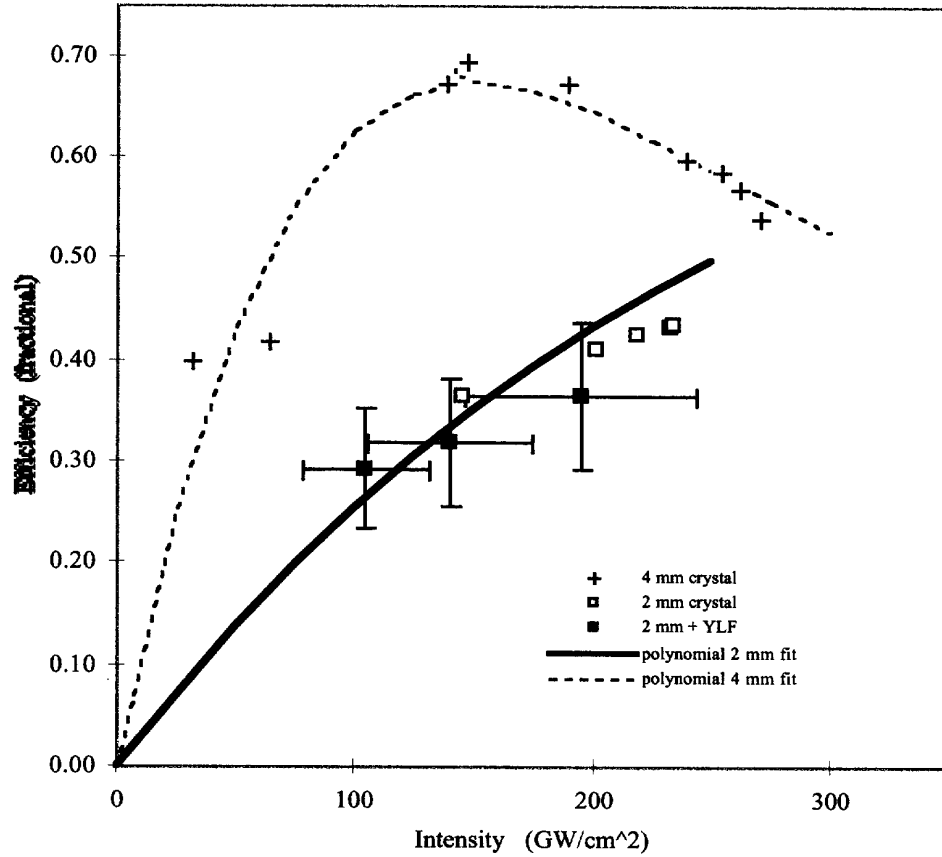


Figure 1. Second harmonic conversion efficiency for 2 and 4 mm thick KDP type 1 crystals as a function of 1054 nm pulse intensity. The fits were generated from a single polynomial (see text) and scaled as crystal thickness squared to fit both sets of data.

$$C(I[\text{GWcm}^{-2}], L[\text{mm}]) = \sum a_n (IL^2)^n \quad (1)$$

for both the 2 and 4 mm crystals at both pulse lengths is used. The fitting coefficients have values of  $a_1=7.379 \times 10^{-04}$ ,  $a_2=-2.804 \times 10^{-07}$ ,  $a_3=4.489 \times 10^{-11}$ ,  $a_4=-3.302 \times 10^{-15}$  and  $a_5=9.181 \times 10^{-20}$  and the fit applies in the range  $5 < IL^2 < 50 \text{ GW}$ .

This method of fitting allows us to extrapolate from the measured data into parameter areas in crystal length and intensity that were not directly measured. For example, figure 2, generated on the basis of the fits, explores the possibilities of using the same and different crystals over a variety of different pulse lengths for fluences that represent the design range for the Vulcan compression gratings. It shows that for the current laser system under normal operating fluences with a 700 fs pulse a 2 mm crystal is the optimum choice. However, there are

significant problems associated with the manufacture of a 2 mm thick crystal with an aperture of sufficient size (150 mm x 90 mm) and of reasonable optical quality. The thinnest commercial crystal available<sup>8)</sup> at the time was 4 mm manufactured with a circular aperture of 157 mm. While not being optimum in terms of frequency doubling efficiency this crystal was the closest match available and was installed on the Vulcan system. A transmission interferogram for this crystal is shown in figure 3. The crystal has a 100 mm chord, which gives the fringe shift visible along the top of the image. The  $\lambda/6$  @ 1053 nm wavefront distortion represents to the best of our knowledge an unparalleled quality for such an aperture thin crystal.

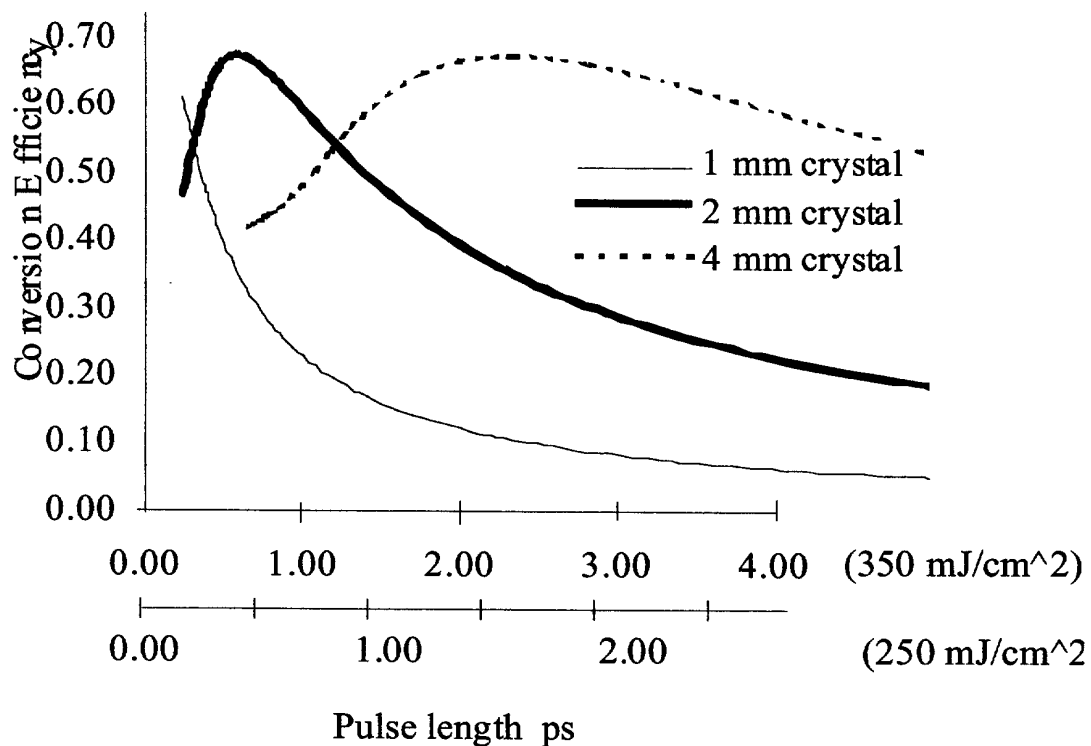


Figure 2. Predicted conversion efficiency for 1, 2 and 4 mm Type 1 frequency crystals as a function of pulse length for incident energy densities of 250 and 350 mJ/cm<sup>2</sup>.

Full beam frequency doubling tests were carried out with this crystal. Calorimeter measurements taken during full energy laser shots showed the same efficiencies to the 4 mm small aperture data shown in figure 1 to within experimental uncertainties. The second harmonic pulse length, measured, using a second order autocorrelator was  $0.68 \pm 0.1$  ps when using a 0.7 ps 1053 nm drive pulse.



## Far Field Quality

Figure 4 illustrates the far field of the frequency doubled beam at a low drive intensity of  $0.1 \text{ GWcm}^{-2}$  (and thus low conversion) and figure 5 illustrates the far field at a high drive intensity of  $200 \text{ GWcm}^{-2}$ . The far field clearly degrades in the high intensity case and fragments into a number of spots distributed in the focal plane. Radial integration of this focal plane distribution indicates that the frequency doubled beam under the conditions of high fundamental intensity is  $\sim 5$  times diffraction limited. As a comparison, previous studies on the fundamental beam have indicated that the beam is approximately 2.5 times diffraction limited. The implication of this result is that there is a significant amount of non-linear phase accumulation, or B-integral<sup>9)</sup>, in the frequency doubled beam, arising both from an incident pump beam carrying a B-integral of 1 and the propagation of the coupled fields through the crystal. To estimate the B-integral in the frequency doubled beam a simple stepwise numerical integration was carried out<sup>10)</sup> using published values of the coefficient of non linear refractive index<sup>11, 12)</sup> This indicated that the expected value of B for the frequency doubled beam under these conditions would be 2.1. Again, previous studies<sup>10)</sup> at 1053 nm have indicated that typically a B greater than 14 is

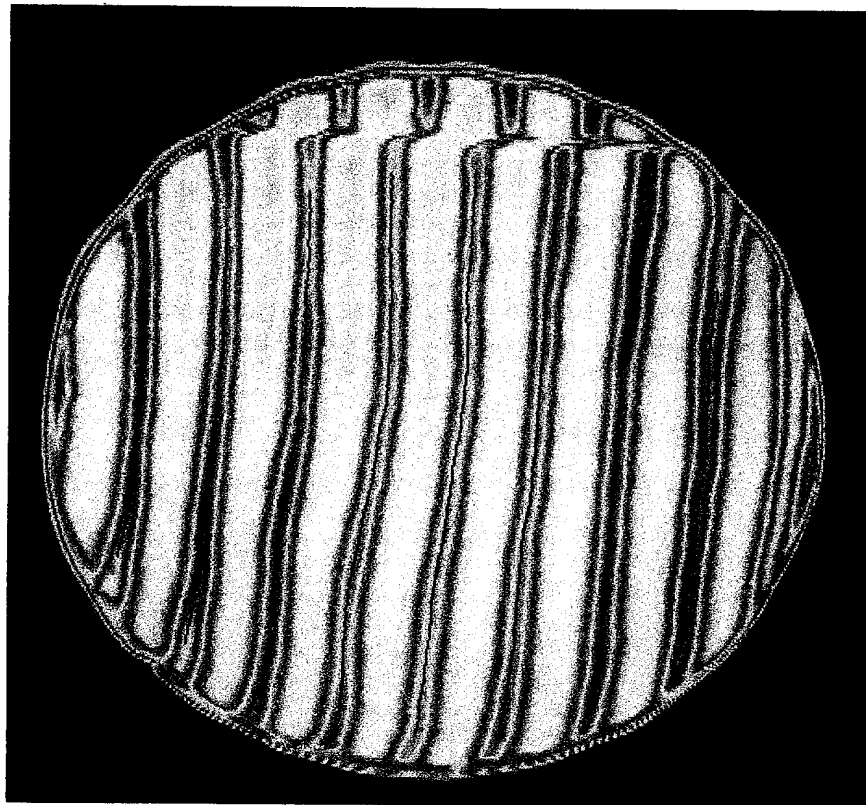


Figure 3. Interferogram of 157 mm diameter 4mm thick KDP crystal.

required to produce a 5 times diffraction limited spot, and even under these relatively high values of  $B$  no fragmentation occurs. It seems unlikely therefore that  $B$ -integral alone is responsible for the break up of the second harmonic far field under these conditions.

## Discussion

The second harmonic conversion efficiency dependence on intensity obtained here are generally in good agreement with the measurements of Chien et al<sup>10)</sup> who used a slightly shorter 500 fs pulse and 26 mm diameter KDP crystals. Chien et al observed no degradation of focusability with type I frequency doubling but did observe some degradation when using a pre-delay scheme and type II doubling. This is similar to the work reported here, where it was only through measurement of the  $\sim 5$  larger beam (and hence more sensitive) frequency doubled far-field that an observation of degradation of focusability was made. In earlier work by Eckardt & Reintjes<sup>13)</sup> it is interesting to note the rapid spectral and temporal pulse break-up introduced by using a crystal, which is thicker than optimal. Their work clearly shows that significant reconversion occurs primarily at the peak of the pulse leading to energy loss and pulse distortion. It is interesting to speculate that in an analogous fashion similar spatial and angular beam perturbations may have been introduced in the present work where the crystal used was thicker than optimum. If the beam break up is due to this, a simple solution might be to slightly detune the crystal delaying peak conversion to the end of the crystal and hence avoiding significant reconversion effects. Although detuning a crystal generally tends to lower the maximum achievable conversion, in the present case where  $B \sim 2$  it should be possible to counterbalance these effects.

Frequency doubling can be considered in an analogous manner to optical parametric amplification as a process in which gain is generated at the frequency doubled wavelength. Phase matching over a range of  $K$  could produce  $\sim 5$  times diffraction limited beam size far-fields which would be in line with the observed measurements. This effect would be more observable for large diameter thin crystals as is the present case. However, it is unclear why break-up in the far-field is observed.

The change in the energy within the wings of the far-field as the irradiance is increased could be due to driving the crystal at saturation in the centre (causing reconversion) of the beam and making the far-field significantly more sensitive to aberrations at the edges of the beam. The far-field would therefore degrade at higher drive irradiances where the effect would be dominant, as it is known that beam quality is poorer in the periphery than at the centre. An adaptive optic based compensation system is presently under design and will be implemented prior to re-testing the system.

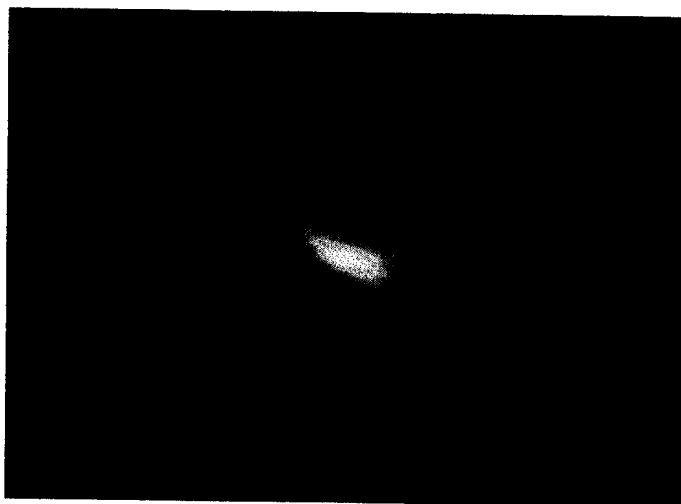


Figure 4. Far-field intensity distribution of the frequency doubled beam obtained at an incident fluence  $0.1 \text{ GWcm}^{-2}$ .



Figure 5. Far-field intensity distribution of the frequency doubled beam obtained at an incident fluence onto the crystal of  $200 \text{ GWcm}^{-2}$ .

## Conclusion

Efficient frequency doubling of the large aperture Vulcan CPA beam was successfully demonstrated with pulses of over 10 TW being delivered to target to study the forward Raman scattering instability in a gas jet. Results of this study are reported in the main body of this report and have been presented internationally.